ISSN 1330-3651 (Print), ISSN 1848-6339 (Online) https://doi.org/10.17559/TV-20210707150253
Original scientific paper

Identifying the Optimal Process Parameter on AA1100 Friction Stir Welded Joints

Premraj YOGARAJ*, Lenin KASIRAJAN

Abstract In this work butt joints were made on AA1100 aluminum alloy using Friction stir welding technique. To obtain strongly bonded weld, the process parameters like profile of tool pin (Cylindrical and threaded tool profile), feed rate of table, inclination of tool, and tool rotation were selected. The parameters thus selected were taken in various levels and in different combinations.The experiments were conducted as per Taguchi L18 mixed orthogonal array design. The process parameters were optimized using Grey Relational Analysis. The optimum process parameters were obtained while using threaded profile with 1200 rpm, tool speed 25 mm/min, movement of the table with 2° tool angle. For this optimized combination, the weld zone produced a maximum of 92.9% of tensile strength, 50.8% of elongation and 91.6% of hardness values compared with the values of the properties of the base material. ANOVA shows that welding speed is a more dominant factor due to the increasing frictional heat generation as well as flow properties of materials in stirred zone.

Keywords: ANOVA, grey relational analysis; hardness; pin profile; Taguchi

1 INTRODUCTION

Materials like aluminium, magnesium and their alloys are employed in many industries for structural, electrical, ship building applications taking advantage of their low density, which leads to improved efficiency, with less fuel consumption. They exhibit high corrosion resistivity, good formability etc., [1]. In the earlier decades conventional metal joining techniques such as Submerged arc welding (SMAW), Electroslag, welding etc, were employed, with some drawbacks. Many researchers have made efforts to improve the optimum performance of the weld joint, especially aluminum and its alloys and revealed that the efficiency is reduced due to dilution, distortion, and residual stresses. Technological advancements, in the recent era have helped manufacturers to improve the quality of welded joints for light metals [2]. Among the latest methods a solid-state friction stir welding technique (FSW) is a promising method [2] which was first patented at The welding institute-Cambridge in 1991 [3]. In this method, joining was carried out in the absence of autogenous, homogeneous and heterogeneous, shielding gases like argon/helium and also it will not create toxic environment [4, 5]. Properties of the joints of similar/dissimilar materials are based on dynamic recrystallization in the weld zone. Maximum deformation happens due to the plasticization in the stirred area [6, 7]. Researchers in FSW have reported that stirring and intermixing of material at the interface region increases with an increase in rotational speed [8]. The grain size in stirred zone is also influenced by increasing rotating speed [9]. Works in friction stir welding of AA1050 alloy have identified that the increment in rotational speed and decrement in traversing speed result in the grain growth in the weld nugget [10]. It has been inferred that medium tool rotation and traversing speed produces finer grains in the stirred zone [11]. Tool angle provides additional thrust force and heat input in the traversing direction of tool [12]. Tool pin is the main factor to stir the materials in the interface region [13]. A notable work on the behaviour of AlSi1MgMn on friction stir welded joints has reported that the weld quality is controlled by the geometry of the tool, traverse speed and rotation speed [14]. Experiments, designed with the help of Taguchi technique at an orthogonal array of L16, were conducted in large numbers on AA5083 plates. A comprehensive ANOVA was performed with the results of conducted experiments, in order to find the optimum process parameters. Outcomes from the analyses reveal that the tilt angle followed in welding and the rotational speed contribute to a good tensile strength [15]. Parametric optimization has been done using Grey relation analysis (GRA) on AA1050 stir welded joints. Micro, and macroscopic examinations showed that fractures occurred at the nugget zone when the levels of parameters were in minimum condition, Taguchi method with GRA provided the optimal combination for a good quality FSW joints [16]. The effects of process parameter such as pin offset, tool offset and position of alloys were analysed using statistical tool ANOVA [17]. Defect free welded joints have been observed in dissimilar aluminum alloys through friction welding methods [18]. The responses on mechanical properties and grain analysis on FSW processed AA2017 plates were studied in detail and the results were explored. Maximum Grain refinement of 8 microns was measured on the contact area of the tool [19]. Dual tool rotational speed in FSW was implemented in the experimentations and it has been identified that the heat input at the weld zone induces important effects in the output characteristics [20]. FSW process was utilized to join Al-Li 2099 materials, parametric analysis was carried out for varied inputs. High UTS was observed at high table traverse speeds. It has been observed that the UTS of joints is almost equal to 75% of the base metal's properties [21]. Influence of tool geometry on FSW process was studied on aluminum alloy, up to 20 microns have been obtained in stirred zone using frustum profile tool [22]. Dissimilar materials of Mg-AZ31B/Al-AA6061 joined using Stir welding process were analyzed and their effects on the process parameters were studied. Plastic deformation occurs intensively at high traverse and rotation of the tool [23]. Symmetric and asymmetric SFSW & DFSW processes were conducted for various tools with different conical angles to enhance the weld strength. During DFSW process the tensile strength obtained at the joint was 84.8% of the base metal and the conical angle was maintained at 10° [24]. Grain size prediction on AA6061 alloy on FSW process was done using ABAQUS and recrystallization changes were observed in the central region [25].

Effects of geometry of tool in FSW were analyzed for UTS on AA7075-T6 material. Taguchi L9 array was used for experimentation with conical and square tool. A maximum UTS of 311.40 Mpa in square tool has been

identified [26]. From the literature review it is obvious that few works were reported on the effect of welding parameters on the properties of weldments. Scanty works were observed in the literature on AA1100 weld joint which has several applications such as bus bar, fabrication works etc., Hence, this work has been carried out to study the influence of each and every parameter on the properties of joints made on AA1100 plates. AA1100 alloys have been chosen owing to their moderate strength and they are widely being applied in sheet metal works. Movement of table/welding speed, geometry of pin profile, and inclination of the tool were taken as welding parameters. For evaluating mechanical properties, tensile and hardness measurements were carried out. To analyze the effects of the parameters, Grey Relational Analysis (GRA) with analysis of variance (ANOVA) has been employed.

2 METHOD OF EXPERIMENTATION

The current research work involves the FSW on AA1100 parent material having dimensions of 100 × 100 × 6 mm thickness.The different elements that constitute the AA1100 alloy and their physical behaviour are given in Tabs. 1 and 2. The Experiments were carried out on FSW machine which was made by RV machine tool Coimbatore. The number of experimental runs is based on Taguchi L18 design. Two different tool profiles, such as cylindrical and threaded tools, were employed. They were made of H13 steel with a shoulder diameter of 18 mm and a length of 100 mm, and a pin diameter of 3.8 mm and a length of 5 mm with FSW process as shown in Fig. 1a, b. Tool pin geometry influencing the FSW process has been demonstrated in previous studies. From earlier studies it has been identified that geometry of tool pin influences the FSW process [27].

Table 1 Alloying elements of the base metal (wt. %)

Zn	Mn	Cu	Si + Fe	Remaining	Al
0.1	0.04	0.1	0.92	0.1	Balance

Table 2 Physical properties of base metal

Yield Strength / Mpa	Ultimate Tensile Strength / MPa	Elongation in / %	Hardness / HV
105	110	12	60

The input/Control welding parameters and their levels show the significant properties on the weld joints. Hence welding parameters such as tool speed, movement of the table, inclination of tool and geometry of tool pin were selected. The three different levels of control parameters used in this experimental investigation are shown in Tab. 3.

Table 3 Process input in Friction stir welding Machine

Parameter	Symbol	Level 1	Level 2	Level 3
Geometry of the tool pin	*P*	Cylinder	Threaded	-
Tool Speed / rpm	*N*	800	1000	1200
Table speed/welding speed / mm/min	*F*	25	35	45
Inclination of tool / °	Ø	1	1.5	2

The performance indicators selected for the study are ultimate tensile strength, percentage of elongation and hardness of the weld. The tensile and hardness specimen was prepared as per ASTM-E8 standards, through wire-cut EDM process shown in Fig. 2. To study the effects in the structure of grains, optical microscopy study was conducted by etching through reagent and polishing through different grades of emery sheets. For observing the tensile strength at the stirred zone of the specimens Electromechanical testing machine of capability (MTS Insight) equal to 100kN was employed.

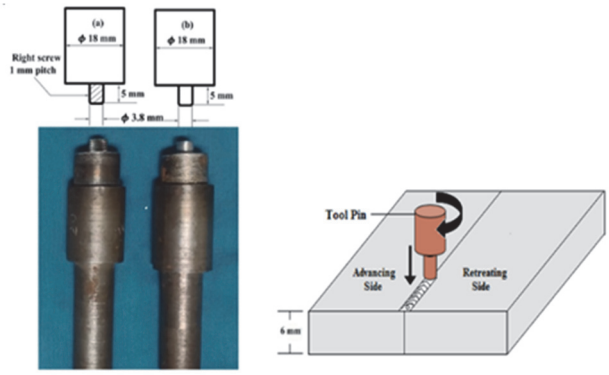

Figure 1 a) Geometry of pin profile; b) Friction stir welding process

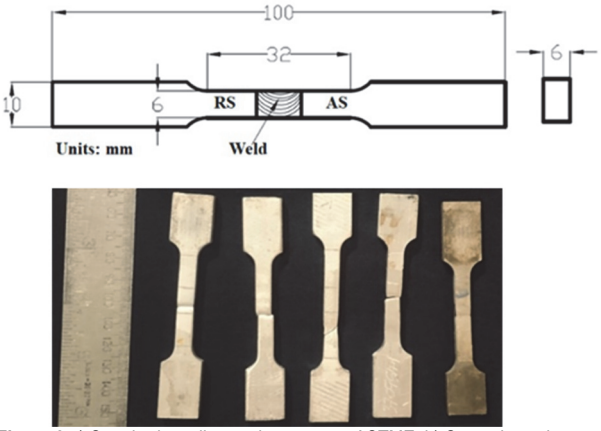

Figure 2 a) Standard tensile specimen as per ASTME; b) Several specimens after tensile testing

The hardness value was measured using Vicker's microhardness tester (Sumitra Enterprises, New Delhi). For each sample, microhardness was measured at three places for each sample and the average was taken. It is essential to optimize the chosen input parameters to obtain maximum performance that can be achieved from the process. Optimization of FSW process parameters has been done by many researchers to obtain maximum tensile strength, hardness, and other mechanical properties using techniques such as GRA, ANOVA, ANN24-27.

3 RESULTS AND DISCUSSION

The investigation has been conducted based on L18 OA design and the results of tensile strength, percentage of elongation, and hardness obtained at different levels of input combinations are given below in Tab. 4. During the tensile test it has been identified that the samples are fractured in weld zone and Thermo-mechanically heat affected zone (TMAZ). The maximum tensile strength of 108.45 MPa has been recorded in 16th trail as shown in Fig. 3a. The parametric combinations are as follows:

Threaded profile, Rotational speed 1200 rpm, traverse speed 25 mm/min and tilt angle 2°. The maximum observed strength may be due to the dynamic recrystallization of grains and minimum traverse speed/movement of the table. They plasticize the interface of metals and this value is found to be 92.9% of the base alloy's tensile strength value. The minimum value of UTS obtained in this experimentation is 68.85 MPa, for trail number 6 (Cylinder profile: 1000 rpm; 45 mm/min; 20 angle). The percentage of elongation of the welded region got decreased considerably as shown in Fig. 3b. The highest percentage of elongation obtained through the optimum combination is 6.1% which is 50.8% of the parent metal value. The large decrement in the value of percentage of elongation can be attributed to the welded region becoming more inhomogeneous due to insufficient recasting of material flow. The maximum value of Vickers hardness obtained from the weld nugget area is 55HVfor an optimum parametric combination. This value is 91.6% of the base material's hardness value.

Table 4 Experimental results

Ex. No.	Geometry of the tool pin *P*	Tool Speed, *N* / rpm	Table movement / Welding speed *F* / mm/min	Inclination of the tool, θ / °	UTS / MPa	% of Elongation	Avg. HV
1	Cylinder	800	25	1	99.45	4.2	52
2	Cylinder	800	35	1.5	82.35	3.7	45
3	Cylinder	800	45	2	71.65	3.1	36
4	Cylinder	1000	25	1	84.65	4.1	47
5	Cylinder	1000	35	1.5	79.45	3.2	38
6	Cylinder	1000	45	2	68.85	2.8	34
7	Cylinder	1200	25	1.5	102.2	5.8	54
8	Cylinder	1200	35	2	92.25	3.8	49
9	Cylinder	1200	45	1	80.65	3.1	42
10	Threaded	800	25	2	90.25	3.9	46
11	Threaded	800	35	1	80.25	3.1	43
12	Threaded	800	45	1.5	74.25	2.9	37
13	Threaded	1000	25	1.5	100.2	5.4	54
14	Threaded	1000	35	2	84.25	3.9	43
15	Threaded	1000	45	1	70.25	3.4	35
16	Threaded	1200	25	2	108.4	6.1	55
17	Threaded	1200	35	1	86.25	3.8	43
18	Threaded	1200	45	1.5	72.25	3.1	35

The nugget shows a series of circular marks throughout the length of the weld and these are also referred to as onion rings [28]. It was observed in the welded joints that the plastically deformed material flowing out from under the shoulder causes "lateral flash". This defect may weaken the behaviour of the weld. The lateral flash occurs in the specimens that were subjected to lower values of tool speed and higher tool feed rates. The lateral flow of material (lateral flash) was found to be less in samples which were joined at higher speeds and lower feeds [29].

4 GRA RESULTS

The proposed research work aims to improve the joint qualities of FS welded AA1100 alloy joints by improving the output quality characteristics at a maximum level. According to the GRA theory, initially all the output quality parameters were normalized for "Larger the better" by using Eq. (1). After normalization, using Eq. (2) *GRC* and *GRG* were calculated and they are presented in Tab. 5.

Table 5 Normalization, *GRC* & *GRG*

Exp. No.	Normalization			Grey Co-efficient			*GRG*
	UTS	% of Elongation	Avg. *HV*	*UTS*	% of Elongation	Avg. *HV*	
1	0.773	0.424	0.857	0.688	0.465	0.778	0.643
2	0.341	0.273	0.524	0.431	0.407	0.512	0.450
3	0.071	0.091	0.095	0.350	0.355	0.356	0.354
4	0.399	0.394	0.619	0.454	0.452	0.568	0.491
5	0.268	0.121	0.190	0.406	0.363	0.382	0.383
6	0.000	0.000	0.000	0.333	0.333	0.333	0.333
7	1.000	0.909	0.952	1.000	0.846	0.913	0.920
8	0.591	0.303	0.714	0.550	0.418	0.636	0.535
9	0.298	0.091	0.381	0.416	0.355	0.447	0.406
10	0.540	0.333	0.571	0.521	0.429	0.538	0.496
11	0.288	0.091	0.429	0.413	0.355	0.467	0.411
12	0.136	0.030	0.143	0.367	0.340	0.368	0.358
13	0.793	0.788	0.952	0.707	0.702	0.913	0.774
14	0.389	0.333	0.429	0.450	0.429	0.467	0.448
15	0.035	0.182	0.048	0.341	0.379	0.344	0.355
16	0.843	1.000	1.000	0.762	1.000	1.000	0.921
17	0.439	0.303	0.429	0.471	0.418	0.467	0.452
18	0.086	0.091	0.048	0.354	0.355	0.344	0.351

The calculated values were ranked with respect to GRG values, from maximum to minimum among the 18 trail experiments with proximity coefficients and the order is: 16 > 7 > 13 > 1 > 8 > 10 > 4 > 17 > 2 > 14 > 11 > 9 > 5 > 12 > 15 > 3 > 18 > 6 which is represented in Tab. 5. It can be observed that the "trail no 16" is producing the best results having the highest grey relational grade of 0.921.

4.1 Response Table for *GRG* and Main Effects Plot for Means

The significance of each welding parameter can be presented by means of the response table and the graph of grey relational grade which are given in Tab. 6 and Fig. 4 respectively. The response graphs of grey relational grade show the change in the response when the factor level goes higher from level 1 to level 3.

Table 6 Response table for *GRG*

Level	Geometry of the tool pin, *P*	Tool Speed, *N* / rpm	Welding speed / Movement of Table, *F* / mm/min	Inclination of the tool, θ / °
1	0.5017	0.4522	0.7075	0.4598
2	0.5074	0.4642	0.4467	0.5395
3	-	0.5973	0.3595	0.5144
Delta	0.0057	0.1451	0.3480	0.0797
Rank	4	2	1	3

Figure 4 Response graph for *GRG*

The results from Tab. 6 and Fig. 4 reveal that the optimal welding parameter set for the welding of Aluminium alloy (AA1100) is $P_2N_3F_1\theta_3$ by applying maximum performance which can be achieved. The results ascertain that the highest tool speed (1200 rpm), lowest movement of the table (25 mm/min) threaded tool pin profile with a maximum tool inclination of 2° produce better quality welded joint.

4.2 Analysis of Variance for *GRG*

Analysis of variance has been used for the obtained *GRG*. Based on the ANOVA results, it has been observed that the welding speed (feed) is the most significant welding parameter followed by the tool rotational speed that has a lesser influence on the multiple performance characteristics and it can be seen in Tab. 7.

Table 7 ANOVA for *GRG*

Source	*DF*	Adj. *SS*	Adj. *MS*	*F*-value	*p*-value	% Contribution
Geometry of Pin Profile, *P*	1	0.000145	0.000145	0.01	0.910	0.024
Tool Speed, *N*	2	0.077795	0.038898	3.58	0.067	12.968
Welding speed, *F*	2	0.393441	0.196721	18.11	0.000	65.584
Inclination of tool, θ	2	0.019926	0.009963	0.92	0.431	3.321
Error	10	0.108596	0.010860	-	-	18.102
Total	17	0.599904	-	-	-	100

The welding speed has the highest contribution (65.6%) to the total variability compared with the other parameters.

4.3 Confirmation Experiment for *GRA* Optimum Combination

It is identified that confirmation test coincides with optimized results. At the highest tool rotational speed of 1200 rpm, lowest welding speed of 25 mm/min and at a tool angle of 2°, the cylindrical tool pin profile provides 108.45 MPa of *UTS*, 5.9% of elongation, and a hardness of 55 HV. It is also seen from the table that the grey relational grade obtained at optimum welding parameter is higher than that of 16th experiment of the orthogonal array. The predicted *GRG* can be estimated by using Eq. (4) given below:

$$\hat{\eta} = \eta_m + \sum_{i=1}^{n} (\overline{\eta}_i - \eta_m) \tag{1}$$

where η_m is total mean of *GRG*, $\overline{\eta}$ is optimal level at each response.

Table 8 Confirmation test

	Initial parameter	Optimal Parameter	
		Prediction	Experiment
Setting level	$P_1N_1F_1\theta_1$	$P_2N_3F_1\theta_3$	$P_2N_3F_1\theta_3$
UTS	99.45	--	102.52
POE	4.2	--	5.9
HV	52	--	57
GRG	**0.643**	**0.836**	**0.923**
Improvement in *GRG* = 0.280			

4.4 ANOVA Results of *UTS*, *POE*, and *HV*

Regression model is developed using statistical software package MINITAB19, based on the selected criterion of process parameters co-efficient are evaluated through observed linear model and their results of ANOVA are presented in Tabs. 9 to 11.

$$\begin{aligned} UTS = {} & 106.3 + 6.7\,P - 15.6\,N - 9.8\,F + 5.4\,\theta + \\ & + 5.27\,N \cdot N + 1.51\,F \cdot F - 2.18\,\theta * \theta - 1.70\,P \cdot N - \\ & - 2.57\,P \cdot F + 0.32\,P \cdot \theta - 1.51\,N \cdot F + 1.82\,N \cdot \theta - \\ & - 0.56\,F \cdot \theta \end{aligned} \tag{2}$$

$$\begin{aligned} POE = {} & 4.09 - 0.28\,P + 0.29N - 1.01F + 1.06\theta + \\ & + 0.012N \cdot N + 0.457F \cdot F - 0.179\theta \cdot \theta + 0.376P \cdot N - \\ & - 0.186P \cdot F - 0.046P \cdot \theta - 0.435N \cdot F + 0.148N \cdot \theta - \\ & - 0.285F \cdot \theta \end{aligned} \tag{3}$$

$$\begin{aligned} HV = {} & 60.9 + 5.2P - 10.7N - 1.2F - 4.3\theta + 2.88N \cdot N + \\ & + 0.64F \cdot F - 0.66\theta \cdot \theta - 0.76P \cdot N - 3.50P \cdot F + \\ & + 1.27P \cdot \theta - 1.19N \cdot F + 2.14N \cdot \theta - 0.15F \cdot \theta \end{aligned} \tag{4}$$

Table 9 ANOVA for *UTS*

Source	*DF*	Adj *SS*	Adj *MS*	*F*-value	*p*-value
Model	13	2167.30	166.715	3.06	0.145
Linear	4	1193.52	298.379	5.48	0.064
P	1	4.06	4.063	0.07	0.798
N	1	120.67	120.666	2.22	0.211
F	1	974.51	974.509	17.90	0.013
θ	1	0.89	0.886	0.02	0.905
Square	3	125.43	41.809	0.77	0.569
N·N	1	103.08	103.076	1.89	0.241
F·F	1	7.62	7.624	0.14	0.727
$\theta \cdot \theta$	1	15.92	15.925	0.29	0.617
2-Way Interaction	6	50.85	8.474	0.16	0.977
P·N	1	7.07	7.066	0.13	0.737
P·F	1	9.68	9.682	0.18	0.695
$P \cdot \theta$	1	0.15	0.147	0.00	0.961
N·F	1	13.12	13.123	0.24	0.649
$N \cdot \theta$	1	19.04	19.036	0.35	0.586
$F \cdot \theta$	1	1.02	1.025	0.02	0.897
Error	4	217.72	54.431	-	-
Total	17	2385.02	-	-	-

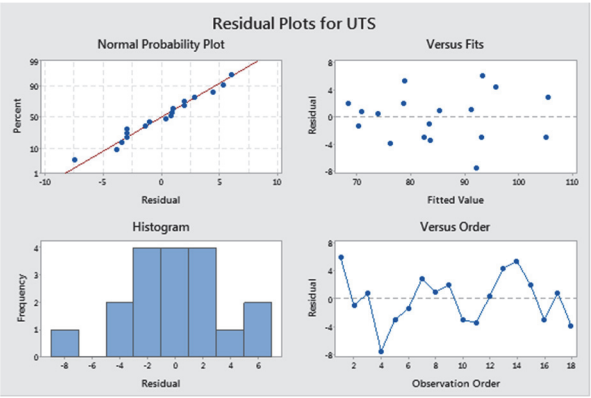

Figure 5 Residual plot for *UTS*

The consistency and dominant parameters are identified with better R^2 value. Predicted R^2 and Adj. R^2 indicate the better outcomes with high accuracy. Based on ANOVA analysis, R^2 has been measured for all three output parameters. For *UTS*, R^2 = 90.87%, *POE*, R^2 =

94.32% and *HV*, R^2 = 91.63%. Based on the R^2, the experimental order showed the high confident level of model with percentage of 90% is significant.

Table 10 ANOVA for *POE*

Source	*DF*	Adj *SS*	Adj *MS*	*F*-value	*p*-value
Model	13	15.4353	1.18733	5.11	0.064
Linear	4	7.3100	1.82750	7.87	0.035
P	1	0.0003	0.00029	0.00	0.973
N	1	1.0544	1.05436	4.54	0.100
F	1	5.7097	5.70974	24.58	0.008
θ	1	0.0001	0.00007	0.00	0.987
Square	3	0.7939	0.26464	1.14	0.434
N·N	1	0.0006	0.00055	0.00	0.963
F·F	1	0.6985	0.69851	3.01	0.158
θ·θ	1	0.1078	0.10779	0.46	0.533
2-Way Interaction	6	1.8386	0.30644	1.32	0.412
P·N	1	0.3439	0.34395	1.48	0.291
P·F	1	0.0507	0.05071	0.22	0.665
P·θ	1	0.0031	0.00306	0.01	0.914
N·F	1	1.0852	1.08523	4.67	0.097
N·θ	1	0.1265	0.12653	0.54	0.501
F·θ	1	0.2633	0.26327	1.13	0.347
Error	4	0.9291	0.23228	-	-
Total	17	16.3644	-	-	-

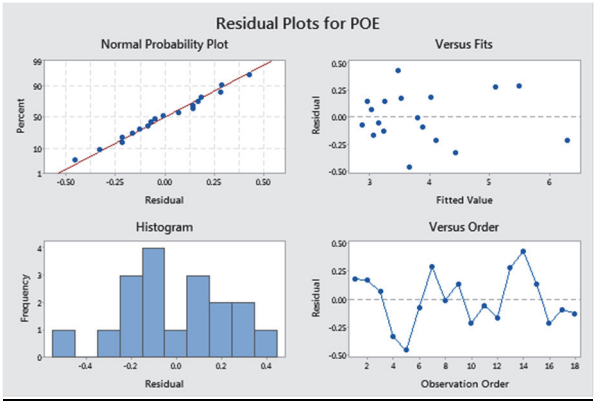

Figure 6 Residual plot for % of Elongation

Table 11 ANOVA for *HV*

Source	*DF*	Adj *SS*	Adj *MS*	*F*-value	*p*-value
Model	13	770.569	59.275	3.36	0.126
Linear	4	375.869	93.967	5.33	0.067
P	1	1.648	1.648	0.09	0.775
N	1	23.270	23.270	1.32	0.315
F	1	304.160	304.160	17.25	0.014
θ	1	8.354	8.354	0.47	0.529
Square	3	33.561	11.187	0.63	0.631
N·N	1	30.769	30.769	1.74	0.257
F·F	1	1.352	1.352	0.08	0.796
θ·θ	1	1.457	1.457	0.08	0.788
2-Way Interaction	6	43.569	7.261	0.41	0.841
P·N	1	1.395	1.395	0.08	0.792
P·F	1	17.885	17.885	1.01	0.371
P·θ	1	2.353	2.353	0.13	0.733
N·F	1	8.119	8.119	0.46	0.535
N·θ	1	26.380	26.380	1.50	0.288
F·θ	1	0.077	0.077	0.00	0.951
Error	4	70.542	17.636		
Total	17	841.111			

The Variance in ANOVA for *UTS*, *POE*, and *HV* is given in Tab. 12. From the table it is identified that movement of the table dominated and influenced 76.11%, 67.82%, and 77.71% on *UTS*, *POE* and *HV* respectively. The residual plot for *UTS*, *POE* and *HV* is shown in Figs. 5 to 7. These figures show that the data closely fall on the straight line which means that the errors are distributed normally.

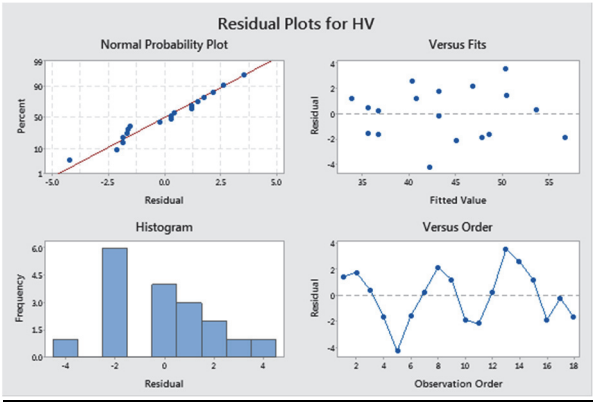

Figure 7 Residual plot for *HV*

Table 12 ANOVA results

Source	*DF*	Adj. *SS*	Adj. *MS*	*F*-value	*p*-value	% of Contribution
Ultimate Tensile Strength (*UTS*)						
Tool Pin Profile, *P*	1	2.90	2.904	0.11	0.749	0.12
Tool rotational Speed, *N*	2	280.56	140.279	5.23	0.028	11.72
Welding speed, *F*	2	1822.55	911.273	33.95	0.000	76.11
Tool Angle, *θ*	2	20.05	10.025	0.37	0.698	0.84
Error	10	268.41	26.841			11.21
Total	17	2394.47				100.00
% of Elongation (*POE*)						
Tool Pin Profile, *P*	1	0.1422	0.1422	0.56	0.473	0.92
Tool rotational Speed, *N*	2	1.7811	0.8906	3.48	0.071	11.49
Welding speed, *F*	2	10.5144	5.2572	20.54	0.000	67.82
Tool Angle, *θ*	2	0.5078	0.2539	0.99	0.405	3.28
Error	10	2.5589	0.2559			16.50
Total	17	15.5044				100.00
Micro Hardness (*HV*)						
Tool Pin Profile, *P*	1	0.889	0.889	0.07	0.793	0.10
Tool rotational Speed, *N*	2	74.778	37.389	3.07	0.091	8.40
Welding speed, *F*	2	691.444	345.722	28.36	0.000	77.71
Tool Angle, *θ*	2	0.778	0.389	0.03	0.969	0.09
Error	10	121.889	12.189			13.70
Total	17	889.778				100.00

ANOVA Tab. 12 shows that the welding parameter, namely the movement of the table has a greater influence on the weld joint, percentage of elongation, and hardness, whereas tool pin profile and tool angle do not affect the properties of joints significantly.

5 MICROSTRUCTURAL STUDY OF WELDED ZONE

The analysis of the experimental results has shown that the welded region cannot attain the property values of the

base material. The attainment of lower values can be attributed to the various defects that occur in the welded area. There are many defects such as lateral flashes, tunnel defects, kissing bond cracks, formation of clusters, precipitation, and development of pores that are associated with FSW process. As this process involves both heat energy and mechanical force, there are many factors that might cause defects.

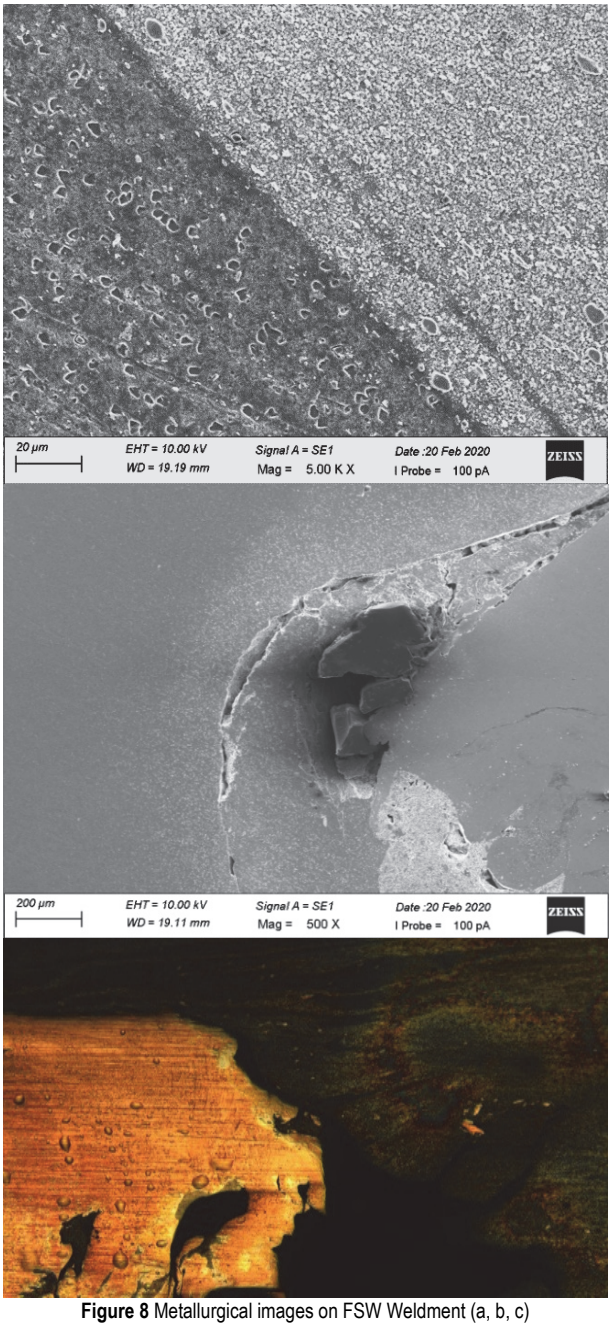

Figure 8 Metallurgical images on FSW Weldment (a, b, c)

The inadequate heat generation and insufficient forward metal flowing i.e. not so substantial metal that flows in the upward direction are the few other intricacies of the process. A few other factors that create such defects are shortfall observed in the plasticization of material at some portions, minimized stirring causing poor metallic bonds, hardening of weld zone material due to excess heat and finally the scarce or excess friction which can significantly affect the quality of the weld [30]. The micro-photograph of the welded zone taken under optical microscope clearly shows the grain refinement in the nugget zone with plastic deformation marks. The nugget zone micro-structure and parent metal are shown in Fig. 8. Compared with the grain orientation of the base material, it is clear that the weld zone contains fine grained micro-structures that are formed due to the recrystallisation temperature and application of mechanical force. The nugget zone normally contains fine grained structures in aluminium alloys. It has been observed by earlier researchers that these are not sub-grain formations but new recrystallized grains formed due to available heat and mechanical compression [31].

Tab. 5 shows that there are no great differences in the properties of weldments while changing the profile of the pin which means that the cylindrical as well as threaded pin profiles generate almost the same amount of heat during joining. On the other hand, Tool Rotational Speed (rpm), Welding Speed (mm/min) and Tool Angle (degree) contribute significantly in the generation of heat during welding. Tool Rotational Speed decides the frictional heat generation in the weld zone. At the same time, Welding Speed decides the contact time and Tool angle controls the thrust force of the tool against the plates [32]. Out of 18 experiments, the seventh experiment gives better tensile strength. This is due to higher rotational rate (1200 rpm), lower welding speed (25 mm/min) and moderate thrust force (1.5 degree) causing high heat generation when compared with the other combination of welding parameters. This heat input produced sufficient plastic deformation, recrystallization, and intermixing which improve the bonding force at the weld zone. As a result, better tensile strength has been observed. This recrystallization process produced finer grains at the stirred zone Fig. 8a which resulted in higher hardness. Finer grains with better bonding force improve the ductile property of the material at the stirred zone. Hence, better elongation property has been established.

Out of 18 experiments, sixth experiment gives poor joint properties (Tab. 4). Moderate rotational rate (1000 rpm), higher welding speed (45 mm/min), and higher thrust force (2 degree) produced very low heat generation during welding. This lower heat input produced insufficient plastic deformation, due to which larger pieces of AA1100 were scratched during the rotation of tool, Fig. 8b. These harder scratched pieces experienced the difficulty in flowing into interface region, which resulted in the poor mixing of materials and the excessive thrust force pulled out the materials excessively in the weld region. This caused poor diffusion and hence, more unmixed regions and volume defects have been observed at the weld nugget, Fig. 8c, and also this low heat input was not enough to produce the recrystallization which produced coarsened grains. As a result, poor hardness is observed. Because of unmixed regions and volume defects in the weld zone, fracture occurred shortly when a tensile load was applied. This is an indication of poor elongation property.

6 CONCLUSIONS

By the application of friction stir welding process with selected input parameters, the optimized conditions were obtained through GRA multi-response optimization technique to attain maximum mechanical properties such

as ultimate tensile strength, percentage elongation, and micro-hardness. The factor that contributes dominantly in the process was also found out by analysis of variance.

ANOVA showed that the parameter welding speed had a greater influence on the joint properties, whereas tool pin profile had the least influence on the joint properties. The micrographical images show the same pattern of grain refinement or recrystallization irrespective of the tool profile being used. All the parameters influence the pocess quite significantly.

The cylindrical pin profile with 1200 rpm rotational rate, 25 mm/min welding speed, and 2° tool angle exhibited better mechanical properties. This was due to the generation of sufficient heat as well as sufficient plastic deformation and effective stirring of materials at weld nugget.

At the same time, the cylindrical pin profile with 1000 rpm rotational rate, 45 mm/min welding speed, and 2° tool angle resulted in poor mechanical properties. This was due to the insufficient heat generation and plastic deformation and poor mixing of materials at weld nugget.

7 REFERENCES

[1] Cantor, B., Grant, P., & Johnston, C. (2008). Automotive Engineering-Lightweight, Functional, and Novel Materials. *Series in Material Science and Engineering.*

[2] Hussain, K. (2010). Evaluation of parameters of friction stir welding for aluminium AA6351 alloy. *International journal of Engineering science and Technology*, *2*(10), 5977-5984,

[3] Thomas, W. M., Nicholas, E. D., Needham, J. C., Murch, M. G., Templesmith, P., & Dawes, C. J. (1991). Improvements relating to Friction Welding. International Patent Application, PCT/GB92/02203 (Patent).

[4] Mishra, R. S., De, P. S. & Kumar, N. (2014). *Frictions Stir Welding and Processing*. Springer International Publishing, Cham, Switzerland. https://doi.org/10.1007/978-3-319-07043-8_9

[5] Lohwasser, D. & Chen, Z. (2010). *Friction stir welding from basics to applications*. Woodhead Publishing Limited, Cambridge, UK. https://doi.org/10.1533/9781845697716

[6] Ashok Kumar, R. & Thansekhar, M. R. (2018). Mechanical and wear properties of friction stir welded dissimilar AA6101-T6 and AA1350 alloys: Effect of offset distance and number of passes. *Journal of Mechanical Science and Technology*, *32*, 3299-3307. https://doi.org/10.1007/s12206-018-0632-8

[7] Raguraman, D., Muruganandam, D., & Kumaraswami Dhas, L. A. (2016). Studies of corrosion on AA 6061 and AZ 61 friction stir welded plates. *Advances in Production Engineering & Management*, *11*(3), 183-191. http://dx.doi.org/10.14743/apem2016.3.219

[8] Dawood, H. I., Mohammed, K. S., & Rajab, M. Y. (2014). Advantages of the green solid state FSW over the conventional GMAW process. *Advances in Materials Scienceand Engineering*, *6*, 1-10. https://doi.org/ 10.1155/2014/105713

[9] Rodriguez, R. I., Jordon, J. B., Allison, P. G., Rushing, T., & Garcia, L. (2015). Microstructure and mechanical properties of dissimilar friction stir welding of 6061-to-7050 aluminum alloys. *Materials and Design*, *83*, 60-65. https://doi.org/10.1016/j.matdes.2015.05.074.

[10] Kasirajan, G., Sathish, R., Ashok Kumar, R., Raghav, G. R., Rao, V. S., & Nagarajan, K. J. (2020). Tensile and wear behaviour of friction stir welded AA5052 and AA6101-T6 aluminium alloys: effect of welding parameters. *Metallurgical Research and Technolgy*, *117*(4), 1-9. https://doi.org/10.1051/metal/2020039

[11] Sato, Y. S., Urata, M., Kokawa, H., & Ikeda, K. (2003). Hall-petch relationship in friction stir welds of equal channel angular pressed aluminium alloys. *Material Science and Engineering A*, *354*, 298-305. https://doi.org/10.1016/S0921-5093(03)00008-X

[12] Ghosh, M., Kumar, K., Kailas, S. V., & Ray, A. K. (2010). Optimization of friction stir welding parameters for dissimilar aluminum alloys. *Materials and Design*, *31*, 3033-3037. https://doi.org/10.1016/j.matdes.2010.01.028

[13] Ashok Kumar, R. & Thansekhar, M. R. (2017). Property evaluation of friction stir welded dissimilar metals: AA6101-T6 and AA1350 aluminium alloys. *Material Science*, *23*(1), 78-83. https://doi.org/10.5755/j01.ms.23.1.14132

[14] Ashok Kumar, R., Muneeswaran, R., Saravana Mohan, M., Rengarajan, S., Raghav, G. R., & Nagarajan, K. J. (2020). Effects of tool pin profile on tensile and wear behaviour of friction stir welded AA6101-T6 and AA1350 alloys. *Metallurgical Research and Technology*, *117*(5), 1-5. https://doi.org/10.1051/metal/202004

[15] Šibalić, N., Vukčević, M., Janjić, M., & Savićević, S. (2016). A Study On Friction Stir Welding Of AlSi1MgMn Aluminium Alloy Plates. *Tehnički vjesnik*, *23*(3), 653-660. https://doi.org/10.17559/TV-20131215184202

[16] Raweni, A., Majstorović, V., Sedmak, A., Tadić, S., & Kirin, S. (2018). Optimization of AA5083 Friction Stir Welding Parameters Using Taguchi Method. *Tehnički vjesnik*, *25*(3), 861-866. https://doi.org/10.17559/TV-20180123115758

[17] Aydin, H., Bayram, A., Esme, U., Kazancoglu, Y., & Guven, O. (2010). Application of Grey Relation Analysis (GRA) and Taguchi Method for The Parametric Optimization Of Friction Stir Welding (FSW) Proces. *Materials and technology*, *44*(4), 205-211.

[18] Ghiasvand, A., Kazemi, M., Mahdipour Jalilian, M., & Ahmadi Rashid, H. (2020). Effects of tool offset, pin offset, and alloys position on maximum temperature in dissimilar FSW of AA6061 and AA5086. *International Journal of Mechanical and Materials Engineering*, 15(1), 1-14. https://doi.org/10.1186/s40712-020-00118-y

[19] Palanivel, R., Laubscher, R. F., Dinaharan, I., & Murugan, N. (2017). Developing a Friction-Stir Welding Window For Joining The Dissimilar Aluminum Alloys AA6351 And AA5083. *Materials and technology*, *51*(1), 5-9. https://doi.org/10.17222/mit.2015.049

[20] Mirjalili, A., Serajzadeh, S., Jamshidi Aval, H., & Kokabi, A. H. (2013). Modeling and Experimental Study on Friction Stir Welding of Artificially Aged AA2017 Plates, *Materials and Manufacturing Processes*, *28*(6), 683-688. https://doi.org/10.1080/10426914.2012.746782

[21] Montazerolghaem, H., Badrossamay, M., Tehrani, A. F., Rad, S. Z., & Esfahani, M. S. (2015). Dual-Rotation Speed Friction Stir Welding: Experimentation and Modeling. *Materials and Manufacturing Processe*, *30*(9), 1109-1114. https://doi.org/10.1080/10426914.2014.973578

[22] Ciskoa, R., Jordon, J. B., Amaro, R. L., Allison, P. G., Wlodarski, J. S., McClell, Z. B., Garcia, L., & Rushing, T. W. *Materials And Manufacturing Processes*, 1069-1076. https://doi.org/10.1080/10426914.2020.1765249

[23] Malik, V., Sanjeev, N. K., Suresh Hebbar, H., & Satish, V. K. (2014). Investigations on the Effect of Various Tool Pin Profiles in Friction Stir Welding Using Finite Element Simulations. *Procedia Engineering*, *97*, 1060-1068. https://doi.org/10.1016/j.proeng.2014.12.384

[24] Jagesvar, V., Ravindra, V. T., Chandraprakash, R., & Rajesh K. K. (2018). Effect of friction stir welding process parameters on Mg-AZ31B/Al-AA6061 joints. *Materials and Manufacturing Processes*, *33*(3), 308-314. https://doi.org/ 10.1080/10426914.2017.1291957

[25] Kazemi, M. & Ghiasvand, A. (2021). Effect of cone angle of cylindrical pin in the SFSW and DFSW on mechanical

properties of AA6061-T6 alloy. *International Journal of Mechanical and Materials Engineering*, *16*(1). https://doi.org/10.1186/s40712-021-00131-9

[26] Ghiasvand, A., Kazemi, M., & Jalilian, M. M. Numerical investigation and prediction of grain size in different friction stir welding areas of AA6061 aluminum alloy, Amirkabir. *Journal of Science and Technology*, 1-3. https://doi.org/10.22060/MEJ.2020.18746.6881

[27] Mohammadi-pour, M., Khodabandeh, A., Mohammadi-pour, S., & Paidar, M. (2016). Microstructure and mechanical properties of jointswelded by friction-stir welding in aluminum alloy 7075-T6 plates for aerospace application.*Rare Metals*, 1-9. https:/doi.org/10.1007/s12598-016-0692-9

[28] Vijayan, S. (2010). Multi objective Optimization of Friction Stir Welding Process Parameters on Aluminum Alloy AA 5083 Using Taguchi-Based Grey Relation Analysis, *Materials and Manufacturing Process*, *25*, 1206-1212. https://doi.org/10.1080/10426910903536782

[29] Vahid, M., Khojastehnezhad, H., & Pourasl, H. (2018). Microstructural characterization and mechanical properties of aluminum 6061-T6 plates welded with copper insert plate (Al/Cu/Al) using friction stir welding. *Transactions of Nonferrous Metals Society of China*, *28*(3), 415-426. https://doi.org/10.1016/S1003-6326(18)64675-8

[30] Ghazvinloo, H. R. & Shadfar, N. (2020). Effect of Friction Stir Welding Parameters on the Quality of Al-6%Si Aluminum Alloy Joints. *Journal of Materials Environment Science*, *11*(5), 751-758.

[31] Rajakumar, S. & Balasubramanian, V. (2012). Multi-Response Optimization of Friction-Stir-Welded AA1100 Aluminum Alloy Joints. *Journal of Materials Engineering and Performance*, *21*(6), 809-822. https://doi.org/10.1007/s11665-011-9979-z

[32] Threadgill, P. L., Leonard, A. J., Shercliff, H. R., & Withers, P. J. (2009). Friction Stir Welding of Aluminium Alloys. *International Materials Reviews*, *54*(2), 49-93. https://doi.org/10.1179/174328009X411136

[33] Zapata, J., Valderrama, J., Hoyos, E., & López, D. (2013). Mechanical Properties Comparison of Friction Stir Welding Butt Joints of AA1100 Made in a Conventional Milling Machine And A FSW Machine. *Dyna*, *80*(182), 115-123.

Contact information

Premraj YOGARAJ
(Corresponding author)
Research Scholar, Anna University,
Lecturer, SA Polytechnic College, Avadi,
Chennai, Tamil Nadu, India
E-mail: premrajsapoly@gmail.com

Lenin KASIRAJAN, Professor
K. Ramakrishnan College of Engineering,
Samayapuram, Trichy, Tamil Nadu, India
E-mail: leninnaga@yahoo.co.in